1 Expression of HIV-1 Intron-Containing RNA in Microglia Induces Inflammatory

2 Responses

- 3
- 4 Running title: HIV RNA-induced innate immune activation in microglia
- 5
- 6 <u>Hisashi Akiyama</u>^{1*}, Sallieu Jalloh¹, Seonmi Park², Maohua Lei¹, Gustavo Mostoslavsky²
- 7 and Suryaram Gummuluru^{1*}
- 8
- 9 ¹Department of Microbiology, ²Center for Regenerative Medicine (CReM), Boston
- 10 University School of Medicine, Boston MA 02118
- 11
- 12 *Corresponding authors
- 13 Hisashi Akiyama, Ph.D.
- 14 Department of Microbiology
- 15 Boston University School of Medicine
- 16 72 E. Concord St., R507
- 17 Boston, MA 02118
- 18 Ph: (617) 358-1773
- 19 Fax: (617) 638-4286
- 20 Email: <u>hakiyama@bu.edu</u>
- 21
- 22 Suryaram Gummuluru, Ph.D.
- 23 Department of Microbiology
- 24 Boston University School of Medicine
- 25 72 E. Concord St., R512
- 26 Boston, MA 02118
- 27 Ph: (617) 358-1774
- 28 Fax: (617) 638-4286
- 29 Email: <u>rgummulu@bu.edu</u>
- 30

31 Abstract

Chronic neuroinflammation is observed in HIV⁺ individuals on suppressive combination 32 33 antiretroviral therapy (cART) and is thought to cause HIV-associated neurocognitive 34 disorders. We have recently reported that expression of HIV intron-containing RNA 35 (icRNA) in productively infected monocyte-derived macrophages induces pro-36 inflammatory responses. Microglia, yolk sac-derived brain-resident tissue macrophages, 37 are the primary HIV-1 infected cell type in the central nervous system (CNS). In this 38 study, we tested the hypothesis that persistent expression of HIV icRNA in primary 39 human microglia induces innate immune activation. We established multiple orthogonal 40 primary human microglia-like cell cultures including peripheral blood monocyte-derived 41 microglia (MDMG) and induced pluripotent stem cell (iPSC)-derived microglia. Unlike 42 MDMG, human iPSC-derived microglia (hiMG), which phenotypically mimic primary CNS 43 microglia, were robustly infected with replication competent HIV-1, and establishment of 44 productive HIV-1 infection and de novo viral gene expression led to pro-inflammatory 45 cytokine production. Blocking of HIV-1 icRNA expression, but not multiply spliced viral 46 RNA, either via infection with virus expressing a Rev-mutant deficient for HIV icRNA 47 nuclear export or infection in the presence of small molecule inhibitor of CRM1-mediated 48 viral icRNA nuclear export pathway, attenuated induction of innate immune responses. 49 These studies suggest that Rev–CRM1-dependent nuclear export and cytosolic sensing 50 of HIV-1 icRNA induces pro-inflammatory responses in productively infected microglia. 51 Novel strategies targeting HIV icRNA expression specifically are needed to suppress 52 HIV-induced neuroinflammation.

Downloaded from http://jvi.asm.org/ on December 16, 2020 by guest

53

54 **Importance**

55 Although peripheral viremia can be effectively suppressed with the advent of highly 56 active anti-retroviral therapy, a significant portion of HIV⁺ individuals still suffer from 57 neurocognitive disorders. Despite suppressive therapy, HIV persists in various tissues 58 including central nervous system (CNS), leading to chronic inflammation, the chief driver 59 of neurocognitive disorders. While persistent infection has been described in CNS-60 resident macrophages, microglia, molecular mechanisms of how HIV infection in 61 microglia contributes to neuronal inflammation have remained unclear. In this study, we 62 used multiple primary human microglia-like cellular platforms and demonstrate that HIV-63 1 intron-containing RNA induces microglial activation and damage. Since current anti-64 retroviral therapy does not suppress HIV-1 transcription, new therapeutics targeting HIV 65 RNA expression may help to treat HIV-associated neurocognitive disorders.

Downloaded from http://jvi.asm.org/ on December 16, 2020 by guest

66

67 Introduction

68 Since the advent of combination antiretroviral therapy (cART), mortality and morbidity of 69 HIV-1 infection has been dramatically reduced. Although prolonged cART can suppress peripheral viremia in HIV⁺ individuals under the detection limit for decades, these 70 71 therapeutic regimens fail to suppress chronic immune activation, the chief driver of HIV-72 associated non-AIDS complications (HANA) including HIV-associated neurocognitive 73 disorders (HAND) (1, 2). Numerous studies have demonstrated that inflammatory 74 markers associated with myeloid cell activation are strongly and selectively predictive of 75 HAND (3). In vivo, persistent HIV infection has been reported in the central nervous 76 system (CNS)-resident macrophages including perivascular macrophages and microglia 77 (4-7). However, molecular mechanisms of how HIV infection in the CNS-resident 78 macrophages contributes to chronic immune activation have remained unclear.

79 Recently, we have shown that expression and Rev-CRM1-dependent nuclear 80 export of HIV intron-containing RNA (icRNA) in productively infected peripheral blood 81 monocyte-derived macrophages (MDMs) is the trigger to induce type I interferon (IFN-I)-82 dependent production of pro-inflammatory cytokines even in the absence of new viral 83 particle production (8). Similar findings have also been reported in monocyte-derived dendritic cells (9), suggesting HIV icRNA expression-induced innate immune activation 84 might be a conserved phenotype in myeloid cells. Numerous studies have documented 85 86 continued presence of HIV RNA in the CSF even after prolonged cART (3, 10-12). Since 87 cART regimens as constituted presently cannot suppress viral RNA expression from 88 integrated proviruses, it is plausible that persistent expression of HIV icRNA in the CNS-89 resident microglia and perivascular macrophages contributes to the chronic 90 inflammatory state in the brain of HIV⁺ individuals on cART.

Z

Journal of Virology

91 Productively infected microglia can contribute to virus persistence and CNS 92 pathology during HIV-1 infection (4, 13), though the extent to which these reservoirs 93 persist and the mechanisms that might allow for virus persistence in these cells in 94 patients on cART remains unclear. HIV infection of microglia has been shown to impact 95 microglial functions including activation status, viability and metabolism (14). In addition, 96 changes in microglial functions have been postulated to contribute to neuropathogenesis 97 by secreting pro-inflammatory cytokines and neurotoxins (15). Activated microglia are 98 also known to cause neurodegeneration directly by damaging synapses or indirectly via 99 activation of other CNS-resident cells such as astrocytes (reviewed in (16)). Microglia 100 play a pivotal role in maintaining brain homeostasis, and microglial dysfunction caused 101 by HIV infection is thought to impact CNS functionality of HIV⁺ individuals on suppressive cART. To date, several mechanisms have been proposed to explain how 102 103 HIV induces microglia activation. For example, HIV proteins Tat, gp120, Nef and Vpr 104 have been shown to activate microglia, leading to alterations in microglial functions and 105 neuronal health (reviewed in (14)). However, the physiological relevance of these 106 findings needs to be carefully considered, since most of the studies have used 107 overexpression of viral proteins or transgenic rodents. Whether such high 108 concentrations of these viral proteins are observed in the CNS of HIV⁺ patients on 109 suppressive therapy requires further investigation. While HIV infection of primary human 110 fetal microglia has been reported (17, 18), these cells are not easily accessible, which 111 preclude detailed investigations of the molecular mechanisms of HIV-induced innate 112 immune activation. Overall, the molecular mechanisms of HIV-induced microglia 113 activation in the CNS remain unclear.

114 In this study, we investigate the role of HIV-1 infection of microglia in promoting 115 neuroinflammation using two model systems, primary monocyte-derived microglia 116 (MDMG) and induced pluripotent stem cell (iPSC)-derived microglia (iCell-MG and 117 hiMG). We report that while HIV-1 infection of MDMGs is attenuated, restriction to 118 infection was alleviated upon SAMHD1 degradation. In contrast, both iCell-MGs and 119 hiMGs were robustly infected with wild type HIV-1, and innate immune activation in 120 these cells was triggered by de novo expression and nuclear export of icRNA via the 121 Rev–CRM1-dependent pathway.

122

Results 123

124 MDMG model of HIV-1 infection in microglia

125 HIV-1 infection of primary human fetal microglia has been reported (17, 18), though 126 these cells are not easily accessible due to ethical and technical issues. To overcome 127 these limitations, microglia-like cells have been generated in vitro from monocytes and 128 characterized extensively (19-22). We derived microglia-like cells from CD14⁺ 129 monocytes by culturing in serum-free conditions in the presence of IL-34 and GM-CSF 130 (Figure 1A). These cells displayed a unique microglia-like ramified morphology (Figure 131 **1B**), as previously reported (19, 20). MDMGs have been shown to display similar 132 morphology to that of human primary microglia and express genes that are highly or uniquely expressed in human microglia (19-23). In agreement with these previous 133 134 findings, expression of P2RY12 and Gas6 mRNAs in MDMGs was significantly 135 enhanced compared to those in donor-matched monocyte-derived macrophages 136 (MDMs) (Figure 1C and D). Furthermore, expression of P2RY12 and IBA-1 in MDMGs 137 was confirmed by immunofluorescence (Figure 1E). We next examined if MDMGs were 138

139

140 quantified by ELISA. While infection of MDMGs resulted in productive infection and release of progeny virions (Figure 1F), the amount of p24^{Gag} in the supernatants was 141 142 very low. Since MDMGs were differentiated from peripheral blood monocytes in GM-143 CSF and IL-34 containing media, and GM-CSF has been shown to alter phosphorylation 144 status of SAMHD1 and render MDMs less susceptible to HIV-1 infection (24), we sought 145 to determine the phosphorylation status of SAMHD1 in MDMGs. Western blotting 146 analysis demonstrated that while total SAMHD1 levels were similar, MDMGs expressed 147 significantly reduced levels of phosphorylated SAMHD1, compared to donor-matched 148 MDMs or THP-1 monocytoid cells (Figure 1G) (25, 26). We next infected MDMGs and donor-matched MDMs with HIV-1 in the absence or presence of SIV_{mac} Vpx containing 149 150 virus-like particles (VLPs) that degrades SAMHD1 (27, 28) and enhances HIV-1 151 infection of myeloid cells (29). In the absence of SIV_{mac} Vpx, MDMGs produced much lower amount of p24^{Gag} in the supernatants than MDMs (Figure 1H). Interestingly, pre-152 treatment of MDMGs with SIV_{mac} Vpx VLPs significantly enhanced p24^{Gag} production 153 154 (Figure 1H), suggesting that abundant expression of anti-viral SAMHD1 in MDMGs 155 restricts efficient infection of these cells by HIV-1.

Downloaded from http://jvi.asm.org/ on December 16, 2020 by guest

susceptible to HIV-1 infection. MDMGs were infected with replication competent CCR5-

tropic HIV-1 (Lai/YU-2env), and p24^{Gag} secretion in the culture supernatants was

156

157 HIV-1 infection induces immune activation in MDMGs

158 We have recently shown that infection of MDMs with HIV-1 induces IFN-I-dependent 159 pro-inflammatory responses (8). To investigate whether HIV-1 infection of microglia 160 induces innate immune activation, total RNA isolated from HIV-1 infected-MDMGs in the 161 presence of SIV_{mac} Vpx VLPs was analyzed with a NanoString human

Ŋ

162 neuroinflammation panel that contains more than 750 target genes covering the core 163 pathways and processes involved in neuroinflammation. Amongst those analyzed, 164 several mRNAs were up-regulated in a HIV-1 infection specific manner, i.e. up-165 regulation was only seen in HIV-infected untreated MDMGs but not in reverse 166 transcriptase inhibitor (efavirenz, EFV)- or integrase inhibitor (raltegravir, Ral)-treated 167 MDMGs (Figure 2A, B and C). Highly up-regulated genes (> mean + 2xSD) compared 168 to mock, EFV- or Ral-treated MDMGs are shown in Figure 2A, 2B and 2C, respectively, 169 which include interferon-stimulated genes (ISGs) (e.g. Siglec1/CD169, RSAD2) and pro-170 inflammatory cytokines (e.g. CXCL10/IP-10, CCL7/MCP-3). To confirm the results from 171 NanoString analysis, IP-10 production in the MDMG culture supernatants was measured 172 by ELISA. We found that IP-10 production was induced upon infection of MDMGs with 173 HIV-1, which was inhibited upon pretreatment of MDMGs with EFV or Ral (Figure 2D). 174 HIV-1 intron-containing RNA (icRNA) export into cytosol via the Rev-CRM1-dependent 175 pathway has previously been shown to induce innate immune activation in MDMs and 176 dendritic cells (8, 9). To investigate the role of HIV-1 icRNA export by the Rev-CRM1-177 dependent pathway in MDMG innate activation, HIV-1 infected MDMGs were treated 178 with a CRM1 inhibitor (KPT-330, selinexor) or MDMGs were infected by an HIV-1 Rev-179 deficient (dominant negative) mutant (M10) (8, 30). While establishment of infection of 180 MDMGs and HIV-1 multiply-spliced RNA expression was not affected by KPT treatment or M10 infection (Figure 2E), production of p24^{Gag} which is transcribed from icRNA, was 181 182 completely inhibited by KPT-330 treatment or in M10-infected MDMGs (Figure 2F). 183 Interestingly, expression of IP-10 mRNA was severely reduced in HIV-1-infected 184 MDMGs upon KPT-330 treatment or in M10-infected MDMGs (Figure 2G). These

185 results suggest that innate immune activation of MDMGs upon HIV-1 infection requires 186 cytoplasmic expression of HIV icRNA exported via the Rev–CRM1-dependent pathway.

187

188 iPSC-derived microglia are highly susceptible to HIV-1 infection

189 Fate mapping analysis suggests that microglia in the brain originate from yolk-sac-190 derived primitive macrophages during embryonic hematopoiesis (31, 32). Unlike other 191 tissue-resident macrophages such as Kupffer cells and alveolar macrophages, microglia 192 are not replenished with circulating bone marrow-derived monocytes during adulthood 193 (33-35). To better model HIV-1 infection of human primary microglia, we tested if human 194 induced pluripotent stem cells (iPSCs)-derived microglia can be infected with HIV-1. We 195 obtained iPSC-derived microglia, iCell Microglia (iCell-MG), from a commercial source 196 (FUJIFILM Cellular Dynamics) which were generated as previously described (36). iCell-197 MGs showed heterogeneous morphology (Figure 3A) and expressed the 198 macrophage/microglia marker IBA-1 (Figure 3B). Flow cytometry analysis revealed 199 robust intracellular expression of the microglia-specific marker P2RY12, and minimal 200 expression on the cell surface (Figure 3C). Immunoblotting analysis revealed that, in 201 contrast to MDMGs, the majority of SAMHD1 was phosphorylated in iCell-MGs (Figure 202 3D). We then infected iCell-MGs with replication competent CCR5-tropic HIV-1/YU-2 and monitored p24^{Gag} production in the culture supernatants over 15 days. We found 203 that iCell-MGs persistently produced p24^{Gag}, which peaked at 6 days p.i. (Figure 3E). 204 Intracellular p24^{Gag} staining revealed that about 20% of iCell-MGs in the culture were 205 206 productively infected at 6 days p.i. (Figure 3F). HIV-1 replication in the infected iCell-MG 207 cultures was inhibited by reverse transcriptase (efavirenz, EFV), integrase (raltegravir, 208 Ral) and CRM1 (KPT-335, verdinexor) inhibitors (Figure 3E and F). To investigate if Downloaded from http://jvi.asm.org/ on December 16, 2020 by guest

209 HIV-1 infection of iCell-MGs induced innate immune activation, we harvested cells on 210 day 6 p.i. and stained them for CD169, a myeloid-cell-specific ISG (37, 38). iCell-MGs 211 upregulated CD169 expression upon infection with HIV-1 (Figure 3G) on both infected 212 cells and on bystander uninfected cells, suggesting that low levels of IFN-I was secreted 213 by infected cells similar to that observed in HIV-1-infected MDMs (8). Expression of 214 CD169 was suppressed by pretreatment of iCell-MGs with RT (EFV), integrase (Ral) 215 and CRM1 (verdinexor) inhibitors (Figure 3H). Furthermore, IP-10 and CCL2 production 216 was induced by productive infection of iCell-MGs by HIV-1 and inhibited upon treatment 217 by EFV, Ral or verdinexor (Figure 3I and J). These results suggest that iPSC-derived 218 microglia are highly susceptible to HIV-1 infection, and that expression and nuclear 219 export of HIV icRNA in infected iCell-MGs triggers innate immune responses in microglia. 220

221 Establishment of iPSC-derived microglia/neuron co-culture system

222 We took advantage of recent descriptions in the literature for generation of microglia 223 from iPSC lines (39). Briefly, iPSC-derived human microglia were derived by co-culturing 224 iPSC-derived yolk-sac primitive macrophages (hiMAC) with iPSC-derived neurons 225 (hiNeuron) (Figure 4A and B) (39). Cells in the hiMG-hiNeuron co-cultures expressed 226 significantly higher levels of mRNA of microglia-specific markers TMEM119 (Figure 4C), 227 CX3CR1 (Figure 4D), and P2RY12 (Figure 4E) compared to those in hiNeuron mono-228 culture hiMACs. Immunofluorescence revealed hiMGs or in expressed 229 macrophage/microglia markers (IBA-1 or TMEM119) (39, 40) and made numerous cell-230 to-cell contacts with neurons as previously reported (Figure 4F) (39). P2RY12 was 231 highly expressed on the cell surface of hiMGs, similar to CNS-resident human microglia

232 (23, 41), and these cells were clearly distinguishable from hiNeuron (tubulin β 3/TUBB3⁺) 233 by flow cytometry (Figure 4G). 234

235 HIV-1 infection of hiMGs induces pro-inflammatory responses

236 hiMG-hiNeuron co-cultures were infected with replication competent HIV-1 Lai/YU-2env, and HIV-1 replication was measured by flow cytometry (intracellular p24^{Gag} expression) 237 238 or ELISA (p24^{Gag} in the culture supernatants). While hiNeurons were not susceptible to 239 HIV-1, hiMGs were robustly infected with HIV-1 in hiMG-hiNeuron co-cultures (Figure 240 5A and B). Furthermore, establishment of infection in hiMG-hiNeuron co-cultures was 241 blocked by pretreatment with EFV and Ral, and anti-CRM1 inhibitor (KPT-330) (Figure 242 **5B**). We detected increasing amounts of p24^{Gag} in the culture supernatants over time 243 (Figure 5C), which is suggestive of persistent virus replication in hiMG-hiNeuron co-244 cultures. HIV-1 infection induced increased production of IP-10 (Figure 5D) and up-245 regulated CCL2 secretion (Figure 5E). HIV-1 infection in microglia has been postulated 246 to lead to neuronal disorder by disrupting microglia viability and functionality (14). To 247 investigate the impact of HIV-1 infection on microglial functionality and neuronal toxicity, HIV-1-infected hiMG-hiNeuron co-cultures were analyzed for microglial and neuronal 248 249 viability by flow cytometry on day 6 p.i. Interestingly, the proportion of live microglia in 250 the co-cultures decreased upon HIV-1 infection over time, which was suppressed upon 251 initiation of infections in the presence of HIV-1 inhibitors (EFV and Ral), suggesting that 252 productive HIV-1 infection, but not exposure to HIV-1 particles alone, affected hiMG 253 viability (Figure 5F). On the other hand, HIV-1 spread in hiMG-hiNeuron co-cultures did 254 not affect the viability of hiNeurons (Figure 5G). These data suggest that hiMGs in the 255 microglia-neuron co-cultures are highly susceptible to HIV-1 infection and that Rev-

Journal of Virology

256 CRM1-dependent nuclear export of HIV icRNA in microglia triggers secretion of pro-

257 inflammatory cytokines, which might contribute to neuroinflammation in vivo.

258

259 Discussion

260 HIV infection and innate immune responses

261 Chronic inflammation is thought to be the chief driver of HAND (2, 42, 43), though 262 underlying mechanisms of persistent neuroinflammation remain unclear. In this study, 263 we demonstrated that HIV-1 infection of microglia induces innate immune activation, 264 resulting in secretion of pro-inflammatory cytokines, up-regulation of ISGs, and microglia 265 cytotoxicity. Considering their long lifespan with self-renewal capacity (31, 44, 45), 266 coupled with the observation that HIV-1⁺ microglia have been detected in cART-267 suppressed individuals (4), it is highly plausible that persistently infected microglia 268 produce pro-inflammatory cytokines and chemokines, such as IFN-I and IP-10, 269 contributing to a chronic state of neuroinflammation. Previous studies have suggested 270 that IFN-I production contributes to cognitive impairments in HIV-1 infection (46) and 271 neurodegenerative diseases (47, 48). Although multiple roles for chemokines in CNS 272 inflammation have been described, CCL2, specifically, has been shown to modulate 273 neuronal death in a mouse model (49, 50). Elevated levels of IP-10 have been observed 274 in several neurodegenerative diseases including in patients with HAND (51) and are 275 known to affect neuronal viability (52, 53). Since we did not find obvious neuronal 276 cytotoxicity in hiMG-hiNeuron co-cultures in 6 days of infection, future studies will be 277 focused on long-term co-cultures and the consequence of persistent HIV-1 infection in 278 microglia on neuronal cytotoxicity such as synaptic loss and dendrite degeneration (54).

279

280 HIV icRNA and innate immune responses

281 While viral proteins such as Tat, Vpr and gp120 have been hypothesized to contribute to 282 HIV-associated neuroinflammation (14), most of these studies have relied on 283 overexpression of viral proteins or transgenic animals. In this study, we showed that 284 HIV-1-infection-induced activation of microglia in all primary cell culture models was 285 triggered by cytoplasmic export of icRNA, since infection with HIV expressing a Rev 286 mutant deficient for CRM1 interaction (M10) was unable to induce innate immune 287 activation (Figure 2), and CRM1 inhibitors suppressed HIV-induced activation in 288 microglia (Figure 2, 3 and 5). We have previously shown that HIV icRNA expression 289 alone induces IFN-I-dependent proinflammatory responses in MDMs, even though HIV 290 icRNA expression does not lead to production of new virions or functional viral proteins including gp120 and Vpr (8). Furthermore, the Rev mutant M10, which fails to induce 291 292 innate immune activation in microglia, expresses multiply-spliced viral RNAs, including 293 those encoding for Tat, suggesting that de novo Tat expression is not the trigger for HIV-294 induced microglia activation. Interestingly, HIV icRNA (gag mRNA) has been detected in 295 the CSF from HIV-1⁺ individuals on cART (3, 10-12), and a highly sensitive RNAScope 296 assay has revealed presence of a significant number of SIV gag mRNA (icRNA) positive 297 cells in the brain of cART-suppressed monkeys (55). We postulate that these viral 298 icRNA expressing cells in the brain, which are most likely microglia, induce pro-299 inflammatory cytokines and affect neuronal health in cART-suppressed individuals. 300 Several drug candidates that suppress expression or stability of HIV icRNA such as Tat 301 and Rev inhibitors (56, 57), or inhibitors that selectively target CRM1-dependent nuclear 302 export of HIV icRNA (58), might have clinical benefit for suppressing HIV icRNA induced 303 aberrant inflammation and incidence of HAND in cART-suppressed patients.

304

305 Establishment of primary human microglia culture system for HIV infection 306 studies.

307 In order to investigate the role of HIV-1 infection of microglia in HIV-1 308 neuropathogenesis, and to overcome the limited access to primary microglia, we 309 employed three different in vitro models of primary microglia in this study: MDMG, iCell-310 MG and hiMG. MDMG expressed microglia-specific markers such as P2RY12 and were 311 poorly susceptible to HIV-1 infection (Figure 1). Since peripheral blood monocytes are 312 readily accessible and the protocol for MDMG generation is relatively simple, MDMG is a 313 reasonable model to study HIV-1 biology in microglia. It should be pointed out that 314 infection of MDMG with HIV-1 in the absence of SAMHD1 antagonism was inefficient (Figure 1). Further optimization of the generation protocol is warranted, for example 315 316 using M-CSF instead of GM-CSF in the differentiation conditions, since GM-CSF has 317 been shown to induce anti-viral SAMHD1 expression in MDMs (24) (Figure 1G). To 318 better mimic the origin of microglia (yolk-sac-derived), we used two independent iPSC-319 derived microglia lines and tested their susceptibility to replication competent HIV-1 in vitro. iCell-MGs are commercially available and expressed microglia markers IBA-1 and 320 321 P2RY12 (Figure 3). It should be noted that as opposed to CNS-resident microglia (23, 322 41), we observed mostly intracellular expression of the microglia-specific marker, 323 P2RY12 in iCell-MGs (Figure 3B). iCell-MGs were highly susceptible to HIV-1 infection 324 (Figure 3), which is in agreement with previous studies using primary fetal microglia (17). 325 While iCell-MG is a powerful tool to study HIV-1 infection in microglia, the inability to 326 genetically manipulate these cells limits their utility in robust mechanistic approaches.

327 The third model we used was hiMG-hiNeuron co-cultures that were generated 328 from iPSCs. This system has numerous advantages: (i) hiMGs are highly susceptible to 329 HIV-1 infection (Figure 5), (ii) establishment of iPSC-derived microglia and neuron co-330 cultures allows for the study of intricate interactions between diverse cell types in the 331 context of viral infection and, importantly, the impact of HIV-infection induced microglia 332 activation can be assessed on autologous neurons, (iii) the purinergic receptor, P2RY12, 333 which detects extracellular nucleotides accompanied with CNS injury and regulates 334 microglial homeostasis (41, 59, 60), and plays an important role in communicating with 335 neighboring neurons to protect their functions (61) is robustly expressed on the hiMG 336 cell surface (in contrast to the mostly intracellular expression of P2RY12 in iCell-MGs), 337 (iv) iPSCs are amenable to gene-editing approaches (62), and (v) iPSC lines generated 338 from somatic cells of various individuals including HIV-infected patients make possible 339 studies of HIV infection of microglia from unique genetic backgrounds and their 340 contribution to human disease. A recently published study (while this manuscript was in 341 preparation) described a new cellular platform that consists of iPSC-derived microglia, 342 neurons and astrocyte tri-cultures (63) and have shown that HIV-1 infection of iPSC-343 microglia in isolation or in tri-cultures resulted in production of pro-inflammatory 344 cytokines including IL-1 β and TNF α . Though the mechanism of induction of pro-345 inflammatory responses in HIV-1 infected microglia was not defined, inflammatory 346 responses were suppressed upon treatment with RT inhibitor (efavirenz) (63). 347 Differentiation protocols for iPSC-derived microglia in this recently published study (63) 348 were similar to those utilized for generation of iCell-MG (iCell Microglia, FUJIFILM 349 Cellular Dynamics) that we tested in this report. While the cytokine-driven differentiation 350 protocol generated iPSC-microglia with similar transcriptional profiles to human primary

Downloaded from http://jvi.asm.org/ on December 16, 2020 by guest

microglia (36, 63), our results suggest that iCell-MGs express low levels of P2RY12 on the cell surface, unlike primary human microglia (23, 41). Since the CNS environment is critical for establishing and maintaining microglial cell identity (64), co-culture-dependent terminal differentiation of iPSC-microglia, as described here and by Takata et al (39), may better model primary microglia in the brain.

356

357 Impact of innate immune activation on homeostatic functions of microglia

358 We have shown that HIV-1 infection of microglia promotes microglia cell death and pro-359 inflammatory cytokine production in the hiMG-hiNeuron co-cultures (Figure 5), though 360 significant cytotoxicity of co-cultured neurons was not observed at the time of harvest (6 361 days p.i.). In contrast, a recent study using non-isogenic iPSC-derived microglia and 362 neurons (from independent lines) demonstrated that infected microglia induce neuronal 363 death, and damaged neurons induce activation of HIV-1 transcription in latently-infected 364 microglia (65). These differences might be the result of divergent experimental setup, as 365 hiMGs in this study were generated by co-culturing hiMACs and hiNeurons from the 366 same iPSC-line, and infections of hiMGs were initiated in co-cultures. Further studies 367 are needed to determine the effects of long-term co-culture of HIV-infected hiMGs and 368 hiNeurons and the consequences of persistent HIV icRNA-induced chronic inflammation 369 on neuronal homeostasis. It has been shown that activation of microglia leads to 370 dysfunctions such as defects in clearing neurotoxins including fibrilar amyloid β and Tau, 371 and promoting a senescent phenotype in microglia (reviewed in (14)). Inclusion of other 372 cell types which have been reported to be HIV-1⁺ in the CNS such as astrocytes and 373 perivascular macrophages (reviewed in (66)) in the hiMG-hiNeuron co-culture might 374 better mimic the brain environment. In addition, human iPSC-derived cerebral organoids

| 375 | with diverse cell types that interact in a 3D environment is an attractive model to study |
|-----|---|
| 376 | HIV neuropathogenesis in vitro (67). Future studies will need to assess the effects of |
| 377 | persistent HIV-1 infection on homeostatic functions of microglia and contribution to |
| 378 | neuronal dysfunction in these 3D cerebral organoid cultures. Finally, our findings |
| 379 | highlight the urgent need to develop novel therapeutic strategies targeting cytosolic HIV |
| 380 | icRNA expression to reduce HIV-induced neuroinflammation and incidence of HAND. |

Downloaded from http://jvi.asm.org/ on December 16, 2020 by guest

381 Materials and Methods

382 Viruses

383 HIV-1 replication competent molecular clones, Lai/YU-2env, single-round reporter virus 384 constructs, LaidenvGFP (GFP in place of the nef orf) and Rev-deficient LaidenvGFP-385 M10, have been described previously (8, 68, 69). Replication competent viruses were 386 derived from HEK293T cells via calcium phosphate-mediated transient transfection (70). 387 Single-round-replication-competent viruses pseudotyped with VSV-G were generated 388 from HEK293T cells via co-transfection of HIV-1∆env proviral plasmids and VSV-G 389 expression plasmid, and the packaging construct (psPAX2), if necessary (70). SIV_{mac} 390 Vpx containing VLPs were generated from HEK293T cells via co-transfection of SIV3⁺, a 391 SIV packaging plasmid containing SIVmac239 Vpx (29), and VSV-G expression plasmid. 392 Virus-containing cell supernatants were harvested 2 days post-transfection, cleared of 393 cell debris by centrifugation (300 x g, 5 min), passed through 0.45 µm filters, and purified 394 and concentrated by ultracentrifugation on a 20% sucrose cushion (24,000 rpm and 4°C 395 for 2 hours with a SW32Ti or SW28 rotor (Beckman Coulter)). The virus pellets were resuspended in PBS, aliquoted and stored at -80 °C until use. The capsid content of 396 397 HIV-1 was determined by a p24^{gag} ELISA (70) and virus titer was measured on TZM-bl 398 by measuring β -gal activity as previously described (71).

399

400 Cell culture

401 HEK293T (ATCC) and TZM-bl (NIH AIDS Reagent Program) were maintained in DMEM
402 (Gibco) containing 10% heat-inactivated FBS (Gibco) and 1% pen/strep (Gibco) (37, 70,
403 72). THP-1 (NIH AIDS Reagent Program) was maintained in RPMI1640 (Gibco)
404 containing 10% FBS and 1% pen/strep (73). In some experiments, THP-1 cells were

Journal of Virology

405 stimulated with PMA (Sigma-Aldrich) for 48 hours at 100 nM. All cell lines have been 406 tested for mycoplasma contamination and confirmed negative. Human iPSC-derived 407 microglia were either purchased (iCell Microglia, FUJIFILM Cellular Dynamics) or 408 generated by us (hiMG, see below). iCell Microglia (iCell-MG) were maintained per the 409 manufacturer's instruction. All the reagents used to maintain iCell-MG are listed below: 410 DMEM/F-12, HEPES no phenol red (Gibco, #11039021), B-27 supplement (Gibco, 411 #17504044), GlutaMAX supplement (Gibco, #35050061), insulin-transferrin-selenium 412 (Gibco, # 41400045), MEM non-essential amino acids (Gibco, #11140050), penicillin-413 streptomycin (Gibco, #15140122), N-2 supplement (Gibco, #17502048), bovine serum 414 albumin (Sigma-Aldrich, #A1470), recombinant human CD200 (ACRO Biosystems, 415 #OX2-H5228), recombinant human IL-34 (PeproTech, #200-34), recombinant human 416 fractalkine (PeproTech, #300-31), human insulin solution (Sigma-Aldrich, #19278), 417 human TGF-β1 (Miltenyi Biotec, #130-095-066), ascorbic acid (Sigma-Aldrich, #A8960), 418 recombinant human M-SCF (PeproTech, #300-25), and 1-Thioglycerol (MTG) (Sigma-419 Aldrich, #M6145).

420

421 Generation of monocyte-derived microglia-like cells and macrophages

To generate monocyte-derived microglia (MDMG), CD14⁺ peripheral blood monocytes positively-isolated with CD14 Micro Beads (Miltenyi Biotec) (68) were seeded on Geltrex (Gibco) coated tissue culture plates and cultured for 12-14 days in RPMI1640 Glutamax (Gibco) supplemented with 1% pen/strep, 100 µg/ml of IL-34 (Peprotech), and human GM-CSF (10 ng per ml, Miltenyi Biotec). Human monocyte-derived macrophages (MDMs) were derived from CD14⁺ peripheral blood monocytes by culturing in RPMI1640 (Gibco) containing 10% heat-inactivated human AB serum (Sigma-Aldrich) and

429 recombinant human M-CSF (20 ng per ml; Peprotech) for 5-6 days and maintained in 430 the same media. 431 432

Generation of human iPSC-derived cells

433 Human iPSCs were generated from human PBMCs by using the STEMCCA 434 polycistronic lentiviral vector (74, 75) followed by the removal of integrated 435 reprogramming cassette using Cre recombinase (76), and were maintained in mTeSR1 436 media (STEMCELL Technologies). Human iPSC-derived primitive macrophages 437 (hiMacs) were generated as previously reported (Figure 4A) (39). Briefly, human iPSC 438 colonies were specified to the mesoderm, and induced into hemangioblast and toward 439 hematopoietic precursors followed by differentiation into primitive macrophages by 440 changing culture media every 2-4 days. After differentiation (Day 26), floating cells were 441 collected and used for FACS as described below. In parallel, human iPSC-derived 442 neurons (hiNeurons) were generated from the same batch of iPSCs as previously 443 reported (39). Human iPSCs were dissociated to single cells, plated onto Matrigel-444 coated 6 well plates, and differentiated into neuronal progenitors (NPCs). NPCs were 445 terminally differentiated into hiNeurons. To generate iPSC-derived microglia cells 446 (hiMGs), CD45⁺ CD11b⁺ CD163⁺ CD14⁺ CX3CR1⁺ hiMacs were sorted by FACS as 447 described below and co-cultured with terminally differentiated hiNeurons for 14 days. All 448 the reagents used to generate iPSC-derived cells are listed below: mTeSR (STEMCELL 449 Technologies, #85850), ReLeSR (STEMCELL Technologies, #05872), DMEM/F-12, 450 HEPES (Gibco, #11330057), IMDM (Gibco, #12440061), Stempro-34 SFM (Gibco, 451 #10639-011), neurobasal (Gibco, #21103049), PBS (Gibco, #14190-144), Ham's F-12 452 nutrient mix (Gibco, #11765054), N2 supplement #17502048), B-27 (Gibco,

453

Downloaded from http://jvi.asm.org/ on December 16, 2020 by guest

454 bovine albumin fraction V (7.5% solution) (Gibco, #15260037), primocin (InvivoGen, 455 #ant-pm-2), GlutaMax (Gibco, #35050061), laminin (Gibco, #23017-015), Matrigel 456 hESC-qualified matrix (Corning, #354277), Matrigel membrane matrix (Corning, 457 #354234), poly-L-ornithine solution (Sigma-Aldrich, #P4957), laminin mouse protein, 458 natural (Gibco, #23017015), human transferrin (Roche, #10-652-202-001), glutamic acid 459 (Sigma-Aldrich, #G1251), ascorbic acid (Sigma-Aldrich, #A4544), SB431542 (Tocris, 460 #1614), Y27632 (ROCK inhibitor) (STEMGENT, #04-0012-02), MTG (Sigma-Aldrich, 461 #M6145), accutase (Gibco, #A1110501), polyornithine (Sigma-Aldrich, #P4957), 462 CHIR99021 (Tocris, #4423/10), y-secretase inhibitor XXI, compound E (Millipore, 463 #565790), recombinant human BDNF (R&D Systems, #248-BD), recombinant human 464 GDNF (R&D Systems, #212-GD), recombinant human BMP-4 (R&D Systems, #314-BP), 465 recombinant human VEGF (R&D Systems, #293-VE), recombinant human EGF (R&D 466 Systems, #236-EG), recombinant human FGF2 (R&D Systems, #233-FB), recombinant human SCF (R&D Systems, #255-SC), recombinant human DKK-1 (R&D Systems, 467 468 #5439-DK), recombinant human IL-3 (R&D Systems, #203-IL), recombinant human IL-6 469 (R&D Systems, #206-IL), and recombinant human M-CSF (R&D Systems, #216-MC).

supplement, serum free (Gibco, #17504044), B27 minus vitamin A (Gibco, #12587010),

470

471 Infection

472 Cells were spinoculated with HIV-1 (1h at RT and 1100 x g) at various multiplicity of 473 infection (MOI, typically 0.5 to 2), cultured for 2-3 hours at 37°C, washed to remove 474 unbound virus particles, and cultured for 3-6 days. Infection was quantified by analyzing 475 p24^{Gag} released into the culture supernatants or GFP expression by flow cytometry (BD 476 LSRII). In some experiments, cells were pretreated prior (at least 30 min) to infection

477 with efavirenz (1 μM, NIH AIDS Reagent Program), raltegravir (30 μM, Selleckchem), or
478 treated 2-3 hours post infection (p.i.) with KPT-330 (1 μM, selinexor, Selleckchem), or
479 KPT-335 (0.1 μM, verdinexor, Selleckchem). DMSO (Sigma-Aldrich) was used as a
480 vehicle control.

481

482 RNA analysis

Total mRNA was isolated from 0.5-1x10⁶ cells using an RNeasy kit (QIAGEN) and 483 484 reverse-transcribed using oligo(dT)₂₀ primer (Superscript III, Invitrogen). Target mRNA 485 was guantified using Maxima SYBR Green (Thermo Scientific) using the following primer 486 P2RY12 (forward: 5'- CTTTCTCATGTCCAGGGTCAG-3', sets: reverse: 5'-487 CTGCAGAGTGGCATCTGGTA-3') GAS6 5'and (forward: 488 CCTTCCATGAGAAGGACCTCGT-3', reverse: 5'-GAAGCACTGCATCCTCGTGTTC-3'). 489 Primer sequences for GAPDH, HIV spliced RNA and IP-10 were described previously 490 (72). For hiMG-hiNeuron co-culture, target mRNA was quantified using TagMan 491 Universal PCR Master Mix (ThermoFisher Scientific) and the following primer/probe 492 sets: Hs99999905_m1 (GAPDH), Hs01922583_s1 (CX3CR1), Hs01881698 s1 493 (P2RY12), and Hs01881698_s1 (P2RY12). The C_T value was normalized to that of 494 GAPDH and represented as a relative value to a control using the $2^{-\Delta\Delta C}_{T}$ method as 495 described (72, 77). NanoSting analysis was performed using a human 496 neuroinflammation kit and total RNAs (100 ng) isolated from MDMGs per the 497 manufacturer's instruction.

498

499 ELISA

,

IP-10 and CCL2 production in culture supernatants was measured with a BD Human IP 10 ELISA Set and a BD Human MCP-1/CCL2 ELISA Set, respectively. To quantitate
 virus production, p24^{Gag} in culture supernatants was quantified by in-house ELISA (8).

503

504 Flow cytometry

To sort CD45⁺ CD11b⁺ CD163⁺ CD14⁺ CX3CR1⁺ hiMacs, cells were stained with 505 506 Fixable Viability Stain 780 (BD Bioscience, #565388) followed by staining with a PE-507 conjugated mouse anti-human CD45 antibody (BD Biosciences, #555483, 1:10), an 508 APC-conjugated anti-human CD11b antibody (BioLegend, #301410, 1:20), a BV421-509 conjugated mouse anti-human CD14 antibody (BD Biosciences, #565283, 1:20), a 510 FITC-conjugated mouse anti-human CD163 antibody (BD Biosciences, #563697, 1:20), 511 and a PerCP/Cy5.5-conjugated anti-human CX3CR1 antibody (BioLegend, #341614, 512 1:20) in the presence of human Fc blocker (BD Bioscience, #564220). Stained cells 513 were sorted with Beckman Coulter MoFlo Astrios. To examine microglia activation, iCell-514 MGs or hiMG-hiNeuron co-cultures were harvested with Cellstripper (Corning), stained 515 with Zombie-NIR (BioLegend, #423105, 1:250) followed by staining with a BV421-516 conjugated mouse anti-P2RY12 antibody (BioLegend, 1:50) in the presence of human 517 Fc Blocker (BD Bioscience, #564220). Cells were fixed with 4% PFA (Boston 518 Bioproducts) for 30 min, permeabilized with Perm/Wash (Invitrogen), and intracellular 519 p24^{Gag} expression was detected as described (72) using a FITC-conjugated mouse antip24^{Gag} monoclonal antibody (KC57, Coulter, # 6604665, 1:25). As for iCell-MGs, cell 520 521 surface CD169 expression was also analyzed using a BV605-conjugated mouse anti-522 CD169 antibody (BioLegend, 1:50). Intracellular tubulin β 3 in the hiMG-hiNeuron co-523 cultures were analyzed with an Alexa 549 or 647-conjugated mouse anti-tubulin ß3

lournal of Virology

524 antibody (TUJ-1, BioLegend, 1:50). Cells were analyzed with BD LSRII (BD). Data was 525 analyzed with FlowJo software (FlowJo).

526

527 Imaging

528 For MDMGs and iCell-MGs, cells cultured in coverslip chambers (LabTekII) were 529 washed and fixed with 4% paraformaldehyde. Cells were then permeabilized with 0.1% 530 TritonX100, and stained with a rabbit anti-P2RY12 antibody (Sigma-Aldrich, HPA014518, 531 1:100), or a rabbit anti-IBA1 antibody (Fujifilm Wako, 019-19741, 1:250). Cells were then 532 stained an Alexa594-conjugated anti-mouse-IgG antibody (Invitrogen, # A-11020, 1:200) 533 and DAPI (Sigma-Aldrich). Cell were analyzed with a Nikon SP5 confocal microscope. 534 hiMG-hiNeuron co-culture was fixed, permeabilized, and stained with an mouse anti-535 beta-Tubulin III antibody (Clone TUJ1, STEMCELL Technologies, #60052, 1:1000), and 536 a rabbit polyclonal anti-TMEM119 antibody (Novus Biologicals, #NBP2-30551, 0.25-2 537 µg/mL), or a goat anti-IBA-1 antibody (Abcam, #ab5076, 1:500), followed by a Alexa 538 Fluor 488-conjugated donkey anti-mouse IgG (Invitrogen, #A21202, 1:500) and an Alexa 539 Fluor 594-conjugated goat anti-rabbit IgG (Invitrogen, #A11012, 1:500) or an Alexa Fluor 540 594-conjugated rabbit anti-goat IgG (Invitrogen, #A11080, 1:500), respectively, and 541 DAPI (NucBlue, Invitrogen). Cells were analyzed with a Keyence BZ-X710 All-in-one 542 Fluorescence Microscope. Images were analyzed with ImageJ (NIH).

543

544 Immunoblot Analysis

545 To assess expression of host proteins, cell lysates containing 15-30 µg total protein

- 546 were separated by SDS-PAGE, transferred to nitrocellulose membranes and the
- 547 membranes were probed with the following antibodies: a mouse anti-SAMHD1 antibody

548 (Abcam, #ab67820, 1:1000) or a rabbit anti-phosphorylated (Thr 592) SAMHD1 antibody
549 (Cell Signaling, #15038, 1:1000), and specific staining visualized with secondary
550 antibodies, goat anti-mouse-IgG-DyLight 680 (Pierce) or a goat anti-rabbit-IgG-DyLight
551 800 (Pierce). As loading controls, actin expression was probed using a rabbit anti-actin
552 antibody (Sigma-Aldrich, A2066, 1:5000). Membranes were scanned with an Odessy
553 scanner (Li-Cor).

554

555 Statistics

All the statistical analysis was performed using GraphPad Prism 8. *P*-values were calculated using one-way ANOVA followed by the Tukey-Kramer post-test (symbols for *p*-values shown with a line) or the Dunnett's post-test (comparing to mock), symbols for *p*-values shown on each column), One sample t-test (comparing two samples, symbols for two-tailed *p*-values shown with a line), or a Wilcoxon signed rank test (comparing two samples, symbols for two-tailed *p*-values shown with a line). Symbols represent, *: *p* < 0.05, **: *p* < 0.01, ***: *p* < 0.001, ****: *p* < 0.0001. No symbol: not significant (*p* ≥ 0.05).

563

564 Data availability

565 The authors declare that the data that support the findings of this study are available 566 within the paper and from the corresponding author upon reasonable request.

567

568 Acknowledgments

569 We thank the BUMC Flow Cytometry Core and the Cellular Imaging Core for technical 570 assistance. This work was supported by NIH grants R01Al064099 (SG), R01DA051889

Ŋ

571 (HA, GM and SG), R01AG060890 (SG), R21NS105837 (SG) and P30Al042853 (SG

572 and HA).

573

574 Author Contributions

575 H.A., G.M., and S.G. designed the experiments. H.A., S.J., M.L, and S.P. performed the

576 experiments and analyzed the data. H.A. and S.G. wrote the manuscript.

577

Accepted Manuscript Posted Online

578 References

579

| 580 581 | 1. | Deeks SG, Tracy R, Douek DC. 2013. Systemic effects of inflammation on health during chronic HIV infection. Immunity 39:633-45. |
|------------|-----|---|
| 582 | 2. | Saylor D, Dickens AM, Sacktor N, Haughey N, Slusher B, Pletnikov M, |
| 583 | | Mankowski JL, Brown A, Volsky DJ, McArthur JC. 2016. HIV-associated |
| 584 | | neurocognitive disorderpathogenesis and prospects for treatment. Nat Rev |
| 585 | | Neurol 12:234-48. |
| 586 | 3. | Peluso MJ, Ferretti F, Peterson J, Lee E, Fuchs D, Boschini A, Gisslen M, Angoff |
| 587 | | N, Price RW, Cinque P, Spudich S. 2012. Cerebrospinal fluid HIV escape |
| 588 | | associated with progressive neurologic dysfunction in patients on antiretroviral |
| 589 | | therapy with well controlled plasma viral load. AIDS 26:1765-74. |
| 590 | 4. | Rappaport J, Volsky DJ. 2015. Role of the macrophage in HIV-associated |
| 591 | | neurocognitive disorders and other comorbidities in patients on effective |
| 592 | | antiretroviral treatment. J Neurovirol 21:235-41. |
| 593 | 5. | Campbell JH, Hearps AC, Martin GE, Williams KC, Crowe SM. 2014. The |
| 594 | | importance of monocytes and macrophages in HIV pathogenesis, treatment, and |
| 595 | | cure. AIDS 28:2175-87. |
| 596 | 6. | Honeycutt JB, Thayer WO, Baker CE, Ribeiro RM, Lada SM, Cao Y, Cleary RA, |
| 597 | | Hudgens MG, Richman DD, Garcia JV. 2017. HIV persistence in tissue |
| 598 | | macrophages of humanized myeloid-only mice during antiretroviral therapy. Nat |
| 599 | | Med doi:10.1038/nm.4319. |
| 600 | 7. | Arainga M, Edagwa B, Mosley RL, Poluektova LY, Gorantla S, Gendelman HE. |
| 601 | | 2017. A mature macrophage is a principal HIV-1 cellular reservoir in humanized |
| 602 | | mice after treatment with long acting antiretroviral therapy. Retrovirology 14:17. |
| 603 | 8. | Akiyama H, Miller CM, Ettinger CR, Belkina AC, Snyder-Cappione JE, |
| 604 | | Gummuluru S. 2018. HIV-1 intron-containing RNA expression induces innate |
| 605 | | immune activation and T cell dysfunction. Nat Commun 9:3450. |
| 606 | 9. | McCauley SM, Kim K, Nowosielska A, Dauphin A, Yurkovetskiy L, Diehl WE, |
| 607 | | Luban J. 2018. Intron-containing RNA from the HIV-1 provirus activates type I |
| 608 | | interferon and inflammatory cytokines. Nat Commun 9:5305. |
| 609 | 10. | Canestri A, Lescure FX, Jaureguiberry S, Moulignier A, Amiel C, Marcelin AG, |
| 610 | | Peytavin G, Tubiana R, Pialoux G, Katlama C. 2010. Discordance between |
| 611 | | cerebral spinal fluid and plasma HIV replication in patients with neurological |
| 612 | | symptoms who are receiving suppressive antiretroviral therapy. Clin Infect Dis |
| 613 | | 50:773-8. |
| 614 | 11. | Dahl V, Peterson J, Fuchs D, Gisslen M, Palmer S, Price RW. 2014. Low levels of |
| 615 | | HIV-1 RNA detected in the cerebrospinal fluid after up to 10 years of suppressive |
| 616 | 4.0 | therapy are associated with local immune activation. AIDS 28:2251-8. |
| 617 | 12. | Garvey LJ, Everitt A, Winston A, Mackie NE, Benzie A. 2009. Detectable |
| 618 | | cerebrospinal fluid HIV RNA with associated neurological deficits, despite |
| 619 | 10 | suppression of HIV replication in the plasma compartment. AIDS 23:1443-4. |
| 620 | 13. | Brown A. 2015. Understanding the MIND phenotype: macrophage/microglia |
| 621 | | inflammation in neurocognitive disorders related to human immunodeficiency |
| 622 | | virus infection. Clin Transl Med 4:7. |

Z

| Downloaded from hi |
|------------------------|
| ttp://jvi.asm.org |
| / on December 16, 2020 |
| , 2020 by guest |

| 623 624 | 14. | Chen NC, Partridge AT, Sell C, Torres C, Martin-Garcia J. 2017. Fate of microglia |
|------------|-----|--|
| 625 626 | 15. | during HIV-1 infection: From activation to senescence? Glia 65:431-446. Song WM, Colonna M. 2018. The identity and function of microglia in |
| 627 | 16. | neurodegeneration. Nat Immunol 19:1048-1058. Li Q, Barres BA. 2018. Microglia and macrophages in brain homeostasis and |
| 628 629 | 17. | disease. Nat Rev Immunol 18:225-242. Cenker JJ, Stultz RD, McDonald D. 2017. Brain Microglial Cells Are Highly |
| 630 | | Susceptible to HIV-1 Infection and Spread. AIDS Res Hum Retroviruses 33:1155- |
| 631 632 | 18. | 1165. Walsh JG, Reinke SN, Mamik MK, McKenzie BA, Maingat F, Branton WG, |
| 633 | 10. | Broadhurst DI, Power C. 2014. Rapid inflammasome activation in microglia |
| 634 | | contributes to brain disease in HIV/AIDS. Retrovirology 11:35. |
| 635 | 19. | Sellgren CM, Sheridan SD, Gracias J, Xuan D, Fu T, Perlis RH. 2017. Patient- |
| 636 | | specific models of microglia-mediated engulfment of synapses and neural |
| 637 | | progenitors. Mol Psychiatry 22:170-177. |
| 638 | 20. | Ohgidani M, Kato TA, Setoyama D, Sagata N, Hashimoto R, Shigenobu K, |
| 639 | | Yoshida T, Hayakawa K, Shimokawa N, Miura D, Utsumi H, Kanba S. 2014. |
| 640 | | Direct induction of ramified microglia-like cells from human monocytes: dynamic |
| 641 | | microglial dysfunction in Nasu-Hakola disease. Sci Rep 4:4957. |
| 642 | 21. | Etemad S, Zamin RM, Ruitenberg MJ, Filgueira L. 2012. A novel in vitro human |
| 643 | | microglia model: characterization of human monocyte-derived microglia. J |
| 644 | ~~ | Neurosci Methods 209:79-89. |
| 645 | 22. | Rawat P, Spector SA. 2017. Development and characterization of a human |
| 646 647 | 22 | microglia cell model of HIV-1 infection. J Neurovirol 23:33-46. |
| 648 | 23. | Butovsky O, Jedrychowski MP, Moore CS, Cialic R, Lanser AJ, Gabriely G, Koeglsperger T, Dake B, Wu PM, Doykan CE, Fanek Z, Liu L, Chen Z, Rothstein |
| 649 | | JD, Ransohoff RM, Gygi SP, Antel JP, Weiner HL. 2014. Identification of a unique |
| 650 | | TGF-beta-dependent molecular and functional signature in microglia. Nat |
| 651 | | Neurosci 17:131-43. |
| 652 | 24. | Badia R, Pujantell M, Riveira-Munoz E, Puig T, Torres-Torronteras J, Marti R, |
| 653 | | Clotet B, Ampudia RM, Vives-Pi M, Este JA, Ballana E. 2016. The G1/S Specific |
| 654 | | Cyclin D2 Is a Regulator of HIV-1 Restriction in Non-proliferating Cells. PLoS |
| 655 | | Pathog 12:e1005829. |
| 656 | 25. | White TE, Brandariz-Nunez A, Valle-Casuso JC, Amie S, Nguyen LA, Kim B, |
| 657 | | Tuzova M, Diaz-Griffero F. 2013. The retroviral restriction ability of SAMHD1, but |
| 658 | | not its deoxynucleotide triphosphohydrolase activity, is regulated by |
| 659 | ~~ | phosphorylation. Cell Host Microbe 13:441-51. |
| 660 | 26. | Cribier A, Descours B, Valadao AL, Laguette N, Benkirane M. 2013. |
| 661 662 | | Phosphorylation of SAMHD1 by cyclin A2/CDK1 regulates its restriction activity |
| 662 663 | 27. | toward HIV-1. Cell Rep 3:1036-43. Hrecka K, Hao C, Gierszewska M, Swanson SK, Kesik-Brodacka M, Srivastava S, |
| 664 | 27. | Florens L, Washburn MP, Skowronski J. 2011. Vpx relieves inhibition of HIV-1 |
| 665 | | infection of macrophages mediated by the SAMHD1 protein. Nature 474:658-61. |
| 666 | 28. | Laguette N, Sobhian B, Casartelli N, Ringeard M, Chable-Bessia C, Segeral E, |
| 667 | 20. | Yatim A, Emiliani S, Schwartz O, Benkirane M. 2011. SAMHD1 is the dendritic- |
| 668 | | and myeloid-cell-specific HIV-1 restriction factor counteracted by Vpx. Nature |
| 669 | | 474:654-7. |
| | | |

Σſ

Journal of Virology

| With a little dendritic cel Malim MH, I HIV-1 Rev t | arrosson-Wuilleme L, Bernaud J, Rigal D, Darlix JL, Cimarelli A help from a friend: increasing HIV transduction of monocyte-de lls with virion-like particles of SIV(MAC). Gene Ther 13:991-4. Bohnlein S, Hauber J, Cullen BR. 1989. Functional dissection of rans-activatorderivation of a trans-dominant repressor of Rev | erived of the |
|--|--|-----------------------------------|
| Ginhoux F, Conway SJ, | II 58:205-14. Greter M, Leboeuf M, Nandi S, See P, Gokhan S, Mehler MF, , Ng LG, Stanley ER, Samokhvalov IM, Merad M. 2010. Fate m reals that adult microglia derive from primitive macrophages. S | |
| Gomez Pero Garner H, T resident ma | diguero E, Klapproth K, Schulz C, Busch K, Azzoni E, Crozet L rouillet C, de Bruijn MF, Geissmann F, Rodewald HR. 2015. T crophages originate from yolk-sac-derived erythro-myeloid Nature 518:547-51. | |
| Hou Y, Li W W, Zhao YY quiescence | Y, Sheng Y, Li L, Huang Y, Zhang Z, Zhu T, Peace D, Quigley C, Qian Z. 2015. The transcription factor Foxm1 is essential for and maintenance of hematopoietic stem cells. Nat Immunol 16 Chen J, Lavin Y, Low D, Almeida FF, See P, Beaudin AE, Lum | the 5:810-8. |
| l, Forsberg l Becher B, S myeloid prog | EC, Poidinger M, Zolezzi F, Larbi A, Ng LG, Chan JK, Greter M amokhvalov IM, Merad M, Ginhoux F. 2015. C-Myb(+) erythro genitor-derived fetal monocytes give rise to adult tissue-reside es. Immunity 42:665-78. | Л, - |
| Thion MS, C intimate jour Abud EM, R | Ginhoux F, Garel S. 2018. Microglia and early brain developme rney. Science 362:185-189. Ramirez RN, Martinez ES, Healy LM, Nguyen CHH, Newman S | A, |
| Madany AM JP, Mortaza | Y, Scarfone VM, Marsh SE, Fimbres C, Caraway CA, Fote GM, I, Agrawal A, Kayed R, Gylys KH, Cahalan MD, Cummings BJ, INI A, Carson MJ, Poon WW, Blurton-Jones M. 2017. iPSC-Del roglia-like Cells to Study Neurological Diseases. Neuron 94:27 | Antel rived |
| Akiyama H, 2014. Virus essential for henipavirus. | Miller C, Patel HV, Hatch SC, Archer J, Ramirez NG, Gummul particle release from glycosphingolipid-enriched microdomains r dendritic cell-mediated capture and transfer of HIV-1 and . J Virol 88:8813-25. | s is |
| system. Nat Takata K, K | , Paulson JC, Varki A. 2007. Siglecs and their roles in the imm Rev Immunol 7:255-66. ozaki T, Lee CZW, Thion MS, Otsuka M, Lim S, Utami KH, Fid alleret B, Chakarov S, See P, Low D, Low G, Garcia-Miralles N | an K, |
| R, Zhang J, Wei TS, Mo Wolf Y, Jung Ginhoux F. 2 Provide a P | Goh CC, Gul A, Hubert S, Lee B, Chen J, Low C, Gul A, Hubert S, Lee B, Chen J, Low I, Shadan NB, k E, Kawanishi S, Kitamura Y, Larbi A, Poidinger M, Renia L, I g S, Onder T, Newell E, Huber T, Ashihara E, Garel S, Pouladi 2017. Induced-Pluripotent-Stem-Cell-Derived Primitive Macrop latform for Modeling Tissue-Resident Macrophage Differentiati | Lum J, Ng LG, MA, phages |

714 40. Bennett ML, Bennett FC, Liddelow SA, Ajami B, Zamanian JL, Fernhoff NB, Mulinyawe SB, Bohlen CJ, Adil A, Tucker A, Weissman IL, Chang EF, Li G, Grant 715 716 GA, Hayden Gephart MG, Barres BA. 2016. New tools for studying microglia in 717 the mouse and human CNS. Proc Natl Acad Sci U S A 113:E1738-46.

670

671

672

673

674

675

676

677

678 679

680 681

682

683 684

685

686

687

688 689

690

691

692

693

694

695

696

697

698

699

700

701

702

703

704

705

706

707

708

709

710

711

712

713

29.

30.

31.

32.

33.

34.

35.

36.

37.

38.

39.

Function. Immunity 47:183-198 e6.

| Accepted Manuscript Posted | | | |
|----------------------------|-----|-----|--|
| pt | | | |
| .Е | 718 | 41. | Moore CS, Ase AR, Kinsara A, Rao VT, Michell-Robinson M, Leong SY, Butovsky |
| S | 719 | | O, Ludwin SK, Seguela P, Bar-Or A, Antel JP. 2015. P2Y12 expression and |
| ы Б | 720 | | function in alternatively activated human microglia. Neurol Neuroimmunol |
| ō | 721 | | Neuroinflamm 2:e80. |
| \leq | 722 | 42. | Klatt NR, Chomont N, Douek DC, Deeks SG. 2013. Immune activation and HIV |
| -0 | 723 | | persistence: implications for curative approaches to HIV infection. Immunol Rev |
| Ŏ | 724 | | 254:326-42. |
| <u>ō</u> | 725 | 43. | Phillips AN, Neaton J, Lundgren JD. 2008. The role of HIV in serious diseases |
| O | 726 | | other than AIDS. AIDS 22:2409-18. |
| Ŏ | 727 | 44. | Ajami B, Bennett JL, Krieger C, Tetzlaff W, Rossi FM. 2007. Local self-renewal |
| \triangleleft | 728 | | can sustain CNS microglia maintenance and function throughout adult life. Nat |
| | 729 | | Neurosci 10:1538-43. |
| | 730 | 45. | Hashimoto D, Chow A, Noizat C, Teo P, Beasley MB, Leboeuf M, Becker CD, |
| | 731 | | See P, Price J, Lucas D, Greter M, Mortha A, Boyer SW, Forsberg EC, Tanaka M, |
| | 732 | | van Rooijen N, Garcia-Sastre A, Stanley ER, Ginhoux F, Frenette PS, Merad M. |
| | 733 | | 2013. Tissue-resident macrophages self-maintain locally throughout adult life with |
| | 734 | | minimal contribution from circulating monocytes. Immunity 38:792-804. |
| | 735 | 46. | Rho MB, Wesselingh S, Glass JD, McArthur JC, Choi S, Griffin J, Tyor WR. 1995. |
| | 736 | | A potential role for interferon-alpha in the pathogenesis of HIV-associated |
| | 737 | 47 | dementia. Brain Behav Immun 9:366-77. |
| | 738 | 47. | Main BS, Zhang M, Brody KM, Kirby FJ, Crack PJ, Taylor JM. 2017. Type-I |
| <u>у</u> б | 739 | | interferons mediate the neuroinflammatory response and neurotoxicity induced by |
| 00 | 740 | 40 | rotenone. J Neurochem 141:75-85. |
| al of Virology | 741 | 48. | Frost GR, Jonas LA, Li YM. 2019. Friend, Foe or Both? Immune Activity in |
| of | 742 | 40 | Alzheimer's Disease. Front Aging Neurosci 11:337. |
| σ | 743 | 49. | Kalehua AN, Nagel JE, Whelchel LM, Gides JJ, Pyle RS, Smith RJ, Kusiak JW, |

Disease. Front Aging Neurosci 11:337. Kalehua AN, Nagel JE, Whelchel LM, Gides JJ, Pyle RS, Smith RJ, Kusiak JW, 143 744 Taub DD. 2004. Monocyte chemoattractant protein-1 and macrophage 745 inflammatory protein-2 are involved in both excitotoxin-induced 746 neurodegeneration and regeneration. Exp Cell Res 297:197-211.

- 747 50. Thompson WL, Karpus WJ, Van Eldik LJ. 2008. MCP-1-deficient mice show 748 reduced neuroinflammatory responses and increased peripheral inflammatory 749 responses to peripheral endotoxin insult. J Neuroinflammation 5:35.
- 750 51. Kolb SA, Sporer B, Lahrtz F, Koedel U, Pfister HW, Fontana A. 1999. 751 Identification of a T cell chemotactic factor in the cerebrospinal fluid of HIV-1-752 infected individuals as interferon-gamma inducible protein 10. J Neuroimmunol 753 93:172-81.
- 754 52. Sui Y, Stehno-Bittel L, Li S, Loganathan R, Dhillon NK, Pinson D, Nath A, Kolson 755 D, Narayan O, Buch S. 2006. CXCL10-induced cell death in neurons: role of 756 calcium dysregulation. Eur J Neurosci 23:957-64.
- 757 Sui Y, Potula R, Dhillon N, Pinson D, Li S, Nath A, Anderson C, Turchan J, 53. 758 Kolson D, Narayan O, Buch S. 2004. Neuronal apoptosis is mediated by CXCL10 759 overexpression in simian human immunodeficiency virus encephalitis. Am J 760 Pathol 164:1557-66.
- 761 54. Ru W, Tang SJ. 2017. HIV-associated synaptic degeneration. Mol Brain 10:40.
- 762 55. Estes JD, Kityo C, Ssali F, Swainson L, Makamdop KN, Del Prete GQ, Deeks SG, 763 Luciw PA, Chipman JG, Beilman GJ, Hoskuldsson T, Khoruts A, Anderson J, 764 Deleage C, Jasurda J, Schmidt TE, Hafertepe M, Callisto SP, Pearson H,
- 765 Reimann T, Schuster J, Schoephoerster J, Southern P, Perkey K, Shang L,

| 766 | | Wietgrefe SW, Fletcher CV, Lifson JD, Douek DC, McCune JM, Haase AT, |
|------------|-----|--|
| 767 768 | | Schacker TW. 2017. Defining total-body AIDS-virus burden with implications for curative strategies. Nat Med 23:1271-1276. |
| 769 | 56. | Wan Z, Chen X. 2014. Triptolide inhibits human immunodeficiency virus type 1 |
| 770 | 50. | replication by promoting proteasomal degradation of Tat protein. Retrovirology |
| 771 | | 11:88. |
| 772 | 57. | Campos N, Myburgh R, Garcel A, Vautrin A, Lapasset L, Nadal ES, Mahuteau- |
| 773 | 07. | Betzer F, Najman R, Fornarelli P, Tantale K, Basyuk E, Seveno M, Venables JP, |
| 774 | | Pau B, Bertrand E, Wainberg MA, Speck RF, Scherrer D, Tazi J. 2015. Long |
| 775 | | lasting control of viral rebound with a new drug ABX464 targeting Rev - mediated |
| 776 | | viral RNA biogenesis. Retrovirology 12:30. |
| 777 | 58. | Gravina GL, Senapedis W, McCauley D, Baloglu E, Shacham S, Festuccia C. |
| 778 | | 2014. Nucleo-cytoplasmic transport as a therapeutic target of cancer. J Hematol |
| 779 | | Oncol 7:85. |
| 780 | 59. | De Simone R, Niturad CE, De Nuccio C, Ajmone-Cat MA, Visentin S, Minghetti L. |
| 781 | | 2010. TGF-beta and LPS modulate ADP-induced migration of microglial cells |
| 782 | | through P2Y1 and P2Y12 receptor expression. J Neurochem 115:450-9. |
| 783 | 60. | Haynes SE, Hollopeter G, Yang G, Kurpius D, Dailey ME, Gan WB, Julius D. |
| 784 | | 2006. The P2Y12 receptor regulates microglial activation by extracellular |
| 785 | | nucleotides. Nat Neurosci 9:1512-9. |
| 786 | 61. | Cserep C, Posfai B, Lenart N, Fekete R, Laszlo ZI, Lele Z, Orsolits B, Molnar G, |
| 787 | | Heindl S, Schwarcz AD, Ujvari K, Kornyei Z, Toth K, Szabadits E, Sperlagh B, |
| 788 | | Baranyi M, Csiba L, Hortobagyi T, Magloczky Z, Martinecz B, Szabo G, Erdelyi F, |
| 789 | | Szipocs R, Tamkun MM, Gesierich B, Duering M, Katona I, Liesz A, Tamas G, |
| 790 | | Denes A. 2019. Microglia monitor and protect neuronal function via specialized |
| 791 | | somatic purinergic junctions. Science doi:10.1126/science.aax6752. |
| 792 | 62. | Hockemeyer D, Jaenisch R. 2016. Induced Pluripotent Stem Cells Meet Genome |
| 793 | | Editing. Cell Stem Cell 18:573-86. |
| 794 | 63. | Ryan SK, Gonzalez MV, Garifallou JP, Bennett FC, Williams KS, Sotuyo NP, |
| 795 | | Mironets E, Cook K, Hakonarson H, Anderson SA, Jordan-Sciutto KL. 2020. |
| 796 | | Neuroinflammation and EIF2 Signaling Persist despite Antiretroviral Treatment in |
| 797 | | an hiPSC Tri-culture Model of HIV Infection. Stem Cell Reports 14:703-716. |
| 798 | 64. | Bohlen CJ, Bennett FC, Tucker AF, Collins HY, Mulinyawe SB, Barres BA. 2017. |
| 799 | | Diverse Requirements for Microglial Survival, Specification, and Function |
| 800 | ~- | Revealed by Defined-Medium Cultures. Neuron 94:759-773 e8. |
| 801 | 65. | Alvarez-Carbonell D, Ye F, Ramanath N, Garcia-Mesa Y, Knapp PE, Hauser KF, |
| 802 | | Karn J. 2019. Cross-talk between microglia and neurons regulates HIV latency. |
| 803 | 00 | PLoS Pathog 15:e1008249. |
| 804 | 66. | Gonzalez-Scarano F, Martin-Garcia J. 2005. The neuropathogenesis of AIDS. |
| 805 | 07 | Nat Rev Immunol 5:69-81. |
| 806 | 67. | Marton RM, Pasca SP. 2019. Organoid and Assembloid Technologies for |
| 807 | | Investigating Cellular Crosstalk in Human Brain Development and Disease. |
| 808 | 60 | Trends Cell Biol doi:10.1016/j.tcb.2019.11.004. |
| 809 810 | 68. | Akiyama H, Ramirez NG, Gudheti MV, Gummuluru S. 2015. CD169-mediated |
| 810 | | trafficking of HIV to plasma membrane invaginations in dendritic cells attenuates efficacy of anti-gp120 broadly neutralizing antibodies. PLoS Pathog 11:e1004751. |
| 011 | | encacy of anti-gp120 broadily neutralizing antibodies. PL05 Patriog 11:e1004751. |

 \leq

| 812 813 814 | 69. | Hatch SC, Archer J, Gummuluru S. 2009. Glycosphingolipid composition of human immunodeficiency virus type 1 (HIV-1) particles is a crucial determinant for dendritic cell-mediated HIV-1 trans-infection. J Virol 83:3496-506. |
|-------------------|-----|--|
| 815 816 | 70. | Puryear WB, Akiyama H, Geer SD, Ramirez NP, Yu X, Reinhard BM, Gummuluru S. 2013. Interferon-inducible mechanism of dendritic cell-mediated HIV-1 |
| 817 818 | 71. | dissemination is dependent on Siglec-1/CD169. PLoS Pathog 9:e1003291. |
| 819 | 11. | Derdeyn CA, Decker JM, Sfakianos JN, Wu X, O'Brien WA, Ratner L, Kappes JC, Shaw GM, Hunter E. 2000. Sensitivity of human immunodeficiency virus type 1 to |
| 820 | | the fusion inhibitor T-20 is modulated by coreceptor specificity defined by the V3 |
| 821 | | loop of gp120. J Virol 74:8358-67. |
| 822 | 72. | Miller CM, Akiyama H, Agosto LM, Emery A, Ettinger CR, Swamstrom RI, |
| 823 | | Henderson AJ, Gummuluru S. 2017. Virion associated Vpr alleviates a post- |
| 824 | | integration block to HIV-1 infection of dendritic cells. J Virol |
| 825 826 | 73. | doi:10.1128/JVI.00051-17. Akiyama H, Ramirez NP, Gibson G, Kline C, Watkins S, Ambrose Z, Gummuluru |
| 827 | 75. | S. 2017. Interferon-Inducible CD169/Siglec1 Attenuates Anti-HIV-1 Effects of |
| 828 | | Alpha Interferon. J Virol 91. |
| 829 | 74. | Park S, Mostoslavsky G. 2018. Generation of Human Induced Pluripotent Stem |
| 830 | | Cells Using a Defined, Feeder-Free Reprogramming System. Curr Protoc Stem |
| 831 | | Cell Biol 45:e48. |
| 832 | 75. | Sommer AG, Rozelle SS, Sullivan S, Mills JA, Park SM, Smith BW, Iyer AM, |
| 833 834 | | French DL, Kotton DN, Gadue P, Murphy GJ, Mostoslavsky G. 2012. Generation of human induced pluripotent stem cells from peripheral blood using the |
| 835 | | STEMCCA lentiviral vector. J Vis Exp doi:10.3791/4327. |
| 836 | 76. | Somers A, Jean JC, Sommer CA, Omari A, Ford CC, Mills JA, Ying L, Sommer |
| 837 | | AG, Jean JM, Smith BW, Lafyatis R, Demierre MF, Weiss DJ, French DL, Gadue |
| 838 | | P, Murphy GJ, Mostoslavsky G, Kotton DN. 2010. Generation of transgene-free |
| 839 | | lung disease-specific human induced pluripotent stem cells using a single |
| 840 | | excisable lentiviral stem cell cassette. Stem Cells 28:1728-40. |
| 841 | 77. | Livak KJ, Schmittgen TD. 2001. Analysis of relative gene expression data using |
| 842 843 | | real-time quantitative PCR and the 2(-Delta Delta C(T)) Method. Methods 25:402- 8. |
| 043 844 | | 0. |
| 044 | | |

Downloaded from http://jvi.asm.org/ on December 16, 2020 by guest

• • •

845

Σ

846 Figure Legends

Figure 1. Monocyte-derived microglia (MDMG) are susceptible to HIV-1 infection.

848 (A) Schematic of MDMG differentiation protocol. (B) Representative image of MDMs or 849 MDMGs differentiated from the same donor. Bars=20 µm. (C, D) Expression of (C) 850 P2RY12 (D) GAS6 mRNA in MDMGs was quantified by gRT-PCR and normalized to 851 that of MDM generated from the same donor. (E) Representative immunofluorescence 852 images of MDMGs stained for nucleus (DAPI, blue) and P2RY12 or IBA-1 (red). Bar=20 853 µm. (F) MDMGs were infected with Lai/YU-2env (replication competent CCR5-tropic HIV-1, MOI=1), and production of p24^{Gag} in the culture supernatant was quantified by 854 855 ELISA (3 dpi). (G) Western blot analysis for total SAMHD1, phosphorylated SAMHD1 856 expression in MDMGs, MDMs and THP-1 cells. Actin was probed as a loading control. 857 +: PMA-treated THP-1, -: unstimulated THP-1. (H) MDMGs and MDMs were infected 858 with HIV-1 (Lai∆envGFP/VSV-G, MOI=2, in the absence or presence of SIV_{mac}239 Vpx VLPs), and production of p24^{Gag} in the culture supernatant was quantified by ELISA (3 859 860 dpi). NT: no-treatment (DMSO), EFV: efavirenz (1µM), Ral: raltegravir (30 µM). The 861 means ± SEM are shown and each symbol represents an independent experiment. P-862 values: One-sample t-test (C, two-tailed), the Wilcoxon matched-pairs signed rank test 863 (D, two-tailed), or one-way ANOVA followed by the Tukey-Kramer post-test (F) or the Dunnett's post-test comparing to mock (**H**). *: *p* < 0.05, **: *p* < 0.01, ***: *p* < 0.001. 864

865

866 Figure 2. HIV-1 infection induces innate immune activation in MDMGs.

867 (A) mRNA expression profiles in MDMGs infected with HIV-1 (Lai∆envGFP/VSV-G,
868 MOI=2, in the presence of SIV_{mac}239 Vpx VLPs) was analyzed using the human
869 neuroinflammation panel (NanoString). Expression of mRNA in HIV-1-infected MDMGs

870 was normalized to that in mock-infected MDMGs (A), in infected MDMGs in the 871 presence of (B) efavirenz or (C) raltegravir, and genes which were expressed greater 872 than the mean+ 2xSD are shown. (D) Production of IP-10 in HIV-1-infected MDMGs 873 (MOI=2, 3 dpi) measured by ELISA. Effects of CRM1 inhibitor (KPT-330) on HIV-1-874 infected MDMGs or infection of MDMGs with a Rev mutant deficient for icRNA nuclear 875 export (Rev*: M10) on (E) viral infection (multiply-spliced viral RNA expression, Revindependent, shown as ΔCT to GAPDH), (F) p24^{Gag} production (Rev-dependent) 876 877 measured by ELISA, or (G) IP-10 mRNA expression (shown as Δ CT to GAPDH). The 878 means ± SEM are shown and each symbol represents an independent experiment. P-879 values: one-way ANOVA followed by the Dunnett's post-test comparing to mock (D-G). *: p < 0.05, **: p < 0.01, ****: p < 0.0001. NT: no treatment (DMSO), EFV: efavirenz (1 880 881 μM), Ral: raltegravir (30 μM), KPT: KPT-330 (Selinexor, 1 μM), Rev*: M10.

882

883 Figure 3. iPSC-derived microglia are highly susceptible to HIV-1 infection

Downloaded from http://jvi.asm.org/ on December 16, 2020 by guest

884 (A) Representative phase-contrast images of iCell-MGs (FUJIFILM Cellular Dynamics). 885 Bar=20 µm. (B) Representative immunofluorescence image of iCell-MGs stained for 886 nucleus (DAPI, blue) and IBA-1 (red). Bar=20 µm. (C) Representative flow cytometry 887 profile of iCell-MGs stained for intracellular and surface P2RY12. (D) Western blot 888 analysis for total SAMHD1, phosphorylated SAMHD1 expression in iCell-MGs, MDMGs, 889 and MDMs. Actin was probed as a loading control. (E) Replication kinetics of HIV-1 in 890 iCell-MGs. Cells were infected with HIV-1 (Lai/YU-2env, replication competent CCR5 tropic HIV-1, MOI=1), and production of p24^{Gag} in the culture supernatant was quantified 891 892 by ELISA. (F-J) iCell-MGs were infected with HIV-1 (Lai/YU-2env, MOI=1), and (F) HIV-1 infection (intracellular p24^{Gag} expression) and (**G**, **H**) CD169 expression were analyzed 893

894 by flow cytometry. Production of proinflammatory cytokines (I) IP-10 and (J) CCL2 in the 895 culture supernatants was measured by ELISA (6 dpi). The means ± SEM are shown and 896 each symbol represents an independent experiment. P-values: one-way ANOVA 897 followed by the Dunnett's post-test comparing to mock (**F**, **H**-**J**), *: p < 0.05, **: p < 0.01, ***: p < 0.001, ****: p < 0.0001. NT: no treatment (DMSO), EFV: efavirenz (1 μM), Ral: 898 899 raltegravir (30 µM), Ver: verdinexor (KPT-335, 0.1 µM).

900

901 Figure 4. Establishment of iPSC-derived microglia/neuron co-culture system.

902 (A) Schematic of hiMG generation by co-culturing hiMAC (volk-sac-derived primitive 903 macrophages) and neurons from human iPSCs. (B) Representative phase-contrast 904 image of hiMGs and hiNeurons co-cultured for 11 days. Bar=50 µm (C-E) Expression of 905 (C) TMEM119, (D) CX3CR1, and (E) P2RY12 mRNA in hiMACs or hiMG-hiNeuron co-906 cultures was quantified by gRT-PCR and normalized to that of hiNeuron solo culture. P-907 values from one-way ANOVA test for C, D and E were 0.0972, 0.0829, and 0.0814, 908 respectively. (F) Representative immunofluorescence images of hiMG-hiNeuron co-909 cultures stained for nucleus (DAPI, blue), neuron (tubulin beta 3: TUBB3, green) and 910 MG markers IBA-1 or TMEM119 (red). Bars=50 µm. (G) Representative flow cytometry 911 profile of hiMG-hiNeuron co-culture stained for neurons (TUBB3) and hiMGs (P2RY12). 912 The means ± SEM are shown and each symbol represents an independent experiment.

913

914 Figure 5. HIV-1 infection of hiMGs in hiMG-hiiNeuron co-cultures induces pro-915 inflammatory responses.

916 hiMG-hiNeuron co-cultures were infected with HIV-1 (Lai/YU-2env: replication 917 competent CCR5 tropic HIV-1, MOI=1). (A, B) HIV-1 infection (intracellular p24^{Gag} 918 expression) was analyzed by flow cytometry. (A) Representative flow cytometry profile is 919 shown, and microglia (P2RY12⁺) and neuron (P2RY12⁻) populations are highlighted with pink and blue, respectively. (B) HIV infected (p24^{Gag+}) cells in microglia (pink in A) were 920 921 calculated. (C) Replication kinetics of HIV-1 in hiMG-hiNeuron co-culture. Co-cultures 922 were infected with HIV-1 (Lai/YU-2env, replication competent CCR5 tropic HIV-1, MOI=1), and production of p24^{Gag} in the culture supernatant was quantified by ELISA. 923 924 Production of proinflammatory cytokines (D) IP-10 and (E) CCL2 was measured by 925 ELISA (6 dpi). Proportion of live cells in (F) microglia (pink in A) and (G) neurons (blue in 926 A) was calculated. The means ± SEM are shown and each symbol represents an 927 independent experiment. P-values: one-way ANOVA followed by the Dunnett's post-test 928 comparing to mock (**B**, **D**-**F**), **: *p* < 0.01, ***: *p* < 0.001, ****: *p* < 0.0001. *P*-value from 929 one-way ANOVA test was 0.9662 for G. NT: no-treatment (DMSO), EFV: efavirenz (1 930 μM), Ral: raltegravir (30 μM), KPT: KPT-330 (selinexor, 1 μM).

Downloaded from http://jvi.asm.org/ on December 16, 2020 by guest

931

Α

P2RY12 mRNA (\log_{10} fold) old O

F

HIV-1 p24^{Gag} (ng/ml)

4

3

2

1

0

mock NT

EFV

CD14⁺ isolation

Day 0

4

3

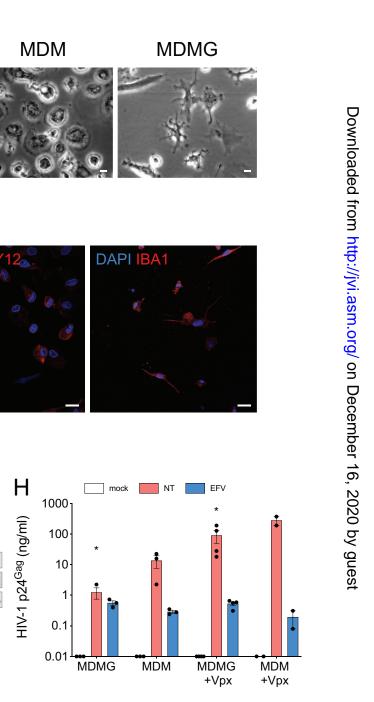
2

1

0

MDM

MDMG



В

Supernatants (p24^{Gag})

3

6 dpi

mRNA analysis (P2RY12 etc.)

Ε

DAPI P

THP-1

Infection

0

12

6

Differentiaion (GM-CSF, IL-34)

9

D

4

3

2

1

0

MDM

Total SAMHD1

p-SAMHD1

Actin

MDMG

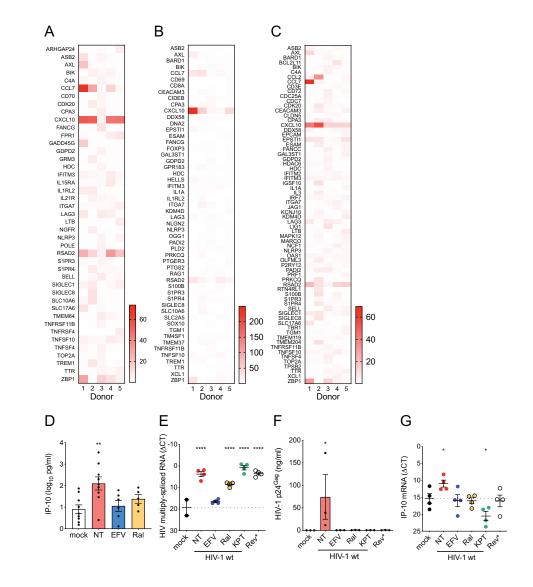
MDMG MDM

GAS6 mRNA (log₁₀ fold)

G

3

 \leq





В

А

Е

HIV-1 p24^{Gag} (ng/ml)

Н

CD169 expression (fold)

40

30

20

10

0

10

8

6

4

2

0Ц

**

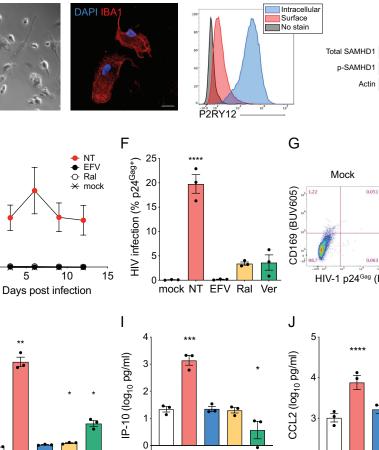
٠

Ţ

mock NT EFV Ral

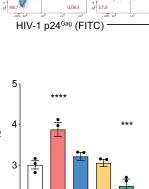
Ver

2



С

mock NT EFV Ral Ver



D

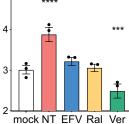
iCell-MG

MDMG MDM

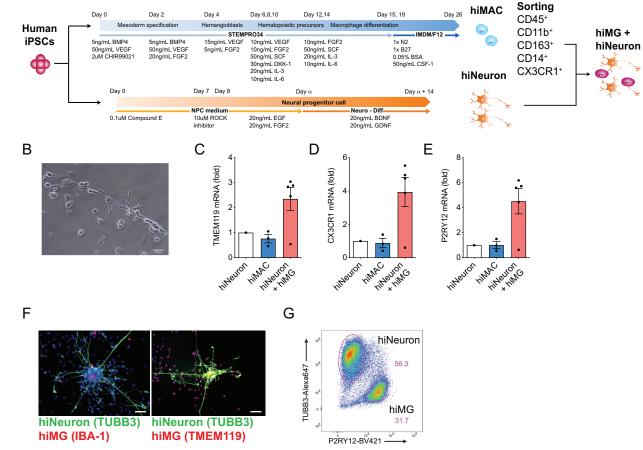
HIV-1

42.0

15.3

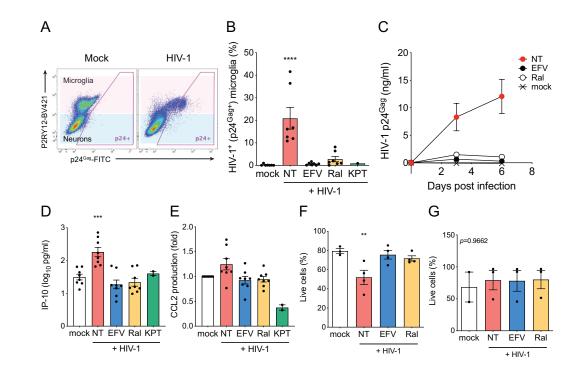


 \sum



А

Downloaded from http://jvi.asm.org/ on December 16, 2020 by guest



Downloaded from http://jvi.asm.org/ on December 16, 2020 by guest